Original Article

Defective Insulin and Acetylcholine Induction of Endothelial Cell–Nitric Oxide Synthase Through Insulin Receptor Substrate/Akt Signaling Pathway in Aorta of Obese Rats

Henrique G. Zecchin,[1] Fernanda B.M. Priviero,[2] Claudio T. Souza,[1] Karina G. Zecchin,[1] Patrícia O. Prada,[1] José B.C. Carvalheira,[1] Licio A. Velloso,[1] Edson Antunes,[2] and Mario J.A. Saad[1]

The actions of acetylcholine (ACh) on endothelium mainly are mediated through muscarinic receptors, which are members of the G protein–coupled receptor family. In the present study, we show that ACh induces rapid tyrosine phosphorylation and activation of Janus kinase 2 (JAK2) in rat aorta. Upon JAK2 activation, tyrosine phosphorylation of insulin receptor substrate (IRS)-1 is detected. In addition, ACh induces JAK2/IRS-1 and IRS-1/phosphatidylinositol (PI) 3-kinase associations, downstream activation of Akt/protein kinase B, endothelial cell–nitric oxide synthase (eNOS), and extracellular signal–regulated kinase (ERK)-1/2. The pharmacological blockade of JAK2 or PI 3-kinase reduced ACh-stimulated eNOS phosphorylation, NOS activity, and aorta relaxation. These data indicate a new signal transduction pathway for IRS-1/PI 3-kinase/Akt/eNOS activation and ERK1/2 by means of JAK2 tyrosine phosphorylation stimulated by ACh in vessels. Moreover, we demonstrate that in aorta of obese rats (high-fat diet), there is an impairment in the insulin- and ACh-stimulated IRS-1/PI 3-kinase pathway, leading to reduced activation with lower protein levels of eNOS associated with a hyperactivated ERK/mitogen-activated protein kinase pathway. These results suggest that in aorta of obese rats, there not only is insulin resistance but also ACh resistance, probably mediated by a common signaling pathway that controls the activity and the protein levels of eNOS. *Diabetes* 56: 1014–1024, 2007

From the [1]Department of Internal Medicine, State University of Campinas, UNICAMP, Campinas, Brazil; and the [2]Department of Pharmacology, State University of Campinas, UNICAMP, Campinas, Brazil.

Address correspondence and reprint requests to Mario J.A. Saad, Department of Internal Medicine, State University of Campinas, UNICAMP, Campinas 13083-970, Brazil. E-mail: msaad@fcm.unicamp.br.

Received for publication 31 August 2005 and accepted in revised form 8 January 2007.

Published ahead of print at http://diabetes.diabetesjournals.org on 17 January 2007. DOI: 10.2337/db05-1147.

ACh, acetylcholine; eNOS, endothelial cell–nitric oxide synthase; ERK, extracellular signal–regulated kinase; GTN, gryceryl trinitrate; IR, insulin receptor; IRS, insulin receptor substrate; JAK2, Janus kinase 2; MAPK, mitogen-activated protein kinase; PI, phosphatidylinositol.

Under physiological conditions, insulin regulates many vascular functions (1,2), including the release of nitric oxide (NO) (3) and the regulation of mRNA expression of matrix proteins (4,5) and constitutive endothelial cell–nitric oxide synthase (eNOS) (6,7). At the molecular level, binding of insulin to its cognate receptor (insulin receptor) results in activation of the insulin receptor's tyrosine kinase activity, which, in turn, phosphorylates tyrosine residues of insulin receptor substrates (IRSs). IRSs are adaptor proteins that transduce signals from the insulin receptor to downstream signaling cascades, including the phosphatidylinositol (PI) 3-kinase/Akt pathway (8,9). In the vasculature, the activation of PI 3-kinase increases serine phosphorylation of Akt, which, in turn, directly phosphorylates eNOS on ser1177 and activates the enzyme, leading to increased NO production (10,11). In addition, a second postreceptor insulin signaling pathway involves the activation of Ras, Raf, mitogen-activated protein and extracellular signal–regulated kinase kinase (MEK), and mitogen-activated protein kinase (MAPK) (extracellular signal–regulated kinase [ERK]-1/2), which is related to cellular growth (12,13). Recent findings (14,15) suggest that impaired IRS-1/PI 3-kinase/Akt/eNOS signal transduction may play a mechanistic role in endothelial dysfunction and in the development of cardiovascular diseases in situations of insulin resistance.

Although insulin is well known in inducing vascular relaxation, the physiological significance of circulating insulin in vascular control is uncertain. Activation of eNOS is generally a calcium-dependent process (16). The vasorelaxation effect of acetylcholine (ACh) is mediated via muscarinic receptors that promote the release of calcium from intracellular stores. This raises the intracellular free-calcium concentration, enabling calcium-calmodulin to bind to eNOS, displacing caveolin-1 and activating eNOS (17).

It recently has been demonstrated that inhibition of PI 3-kinase by Wortmannin attenuated ACh-induced dilation of the basilar artery in vivo (18), raising the hypothesis that cholinergic agonists also may signal through classical tyrosine kinase pathways. However, ACh acts through a G protein–coupled receptor, which does not have intrinsic tyrosine kinase activity. Previous reports (19–22) have demonstrated that other hormones that act through G

protein–coupled receptors, including angiotensin II, vasopressin, and leutinizing hormone, can induce tyrosine phosphorylation of cytoplasmic proteins, including IRSs. Angiotensin II activates Janus kinase 2 (JAK2), a member of the JAK family, and probably uses this kinase to induce several intracellular protein tyrosine phosphorylations.

In this study, we evaluated the ability of ACh to activate JAK2 and to induce the tyrosine phosphorylation of IRS-1 as well as IRS-1/PI 3-kinase association and the phosphorylation of Akt and eNOS in rat aorta. We also compared the activation of IRS-1/PI 3-kinase/Akt/eNOS pathway in response to both ACh and insulin in aorta from normal rats and from an animal model of diet-induced obesity and insulin resistance (i.e., rats fed a high-fat diet for 60 days).

RESEARCH DESIGN AND METHODS

Experimental animals and cells. Eight-week-old male Wistar rats were obtained from the State University of Campinas Central Animal Breeding Center (Campinas, Brazil), divided into two groups with similar body weights (230 ± 25 g), and assigned to receive two types of diet: a standard rodent diet or a high-fat diet for 60 days. The high-fat diet totals 5.4 kcal/g (38.5% carbohydrate, 15% protein, and 46.5% fat), as opposed to the 3.8 kcal/g (70% carbohydrate, 20% protein, and 10% fat) of the standard rodent diet (23). Animals were allowed free access to diet and water ad libitum. At the end of the diet period, body weight and epididymal, perirenal, and mesenteric fat were measured. Food was withdrawn 12 h before the experiments. Blood samples were taken for measuring plasma concentration of total and HDL cholesterol, triacylglycerol, insulin, and plasma glucose (24,25). Rabbit aortic endothelial cells (26) were maintained in F12 medium (Cultilab, Campinas, Brazil) containing 1.2 g/l sodium bicarbonate, 2.5 mmol/l L-glutamine, 15 mmol/l HEPES, and 0.5 mmol/l sodium pyruvate and supplemented with 10% fetal bovine serum (Cultilab), 100 μg/ml gentamicin (Cultilab), 100 IU/ml penicillin (Cultilab), and 100 mg/ml streptomycin (Cultilab) at 37°C in a humidified atmosphere of 5% CO_2. All experiments involving animals were approved by the ethics committee at the State University of Campinas.

All antibodies were from Santa Cruz Biotechnology (Santa Cruz, CA), except anti–phospho-Akt^{ser473}, which was obtained from New England Biolabs (Beverly, MA). Human recombinant insulin was from Eli Lilly (Indianapolis, IN). Routine reagents were from Sigma Chemical (St. Louis, MO), unless specified elsewhere. [^{125}I]Protein A was from Amersham (Little Chalfont, U.K.). Protein A-sepharose MB was from Pharmacia Biotech (Uppsala, Sweden). Nitrocellulose (BA85; 0.2 μm) was from Schleicher & Schuell (Keene, NH). The PI 3-kinase inhibitor LY294002 (Calbiochem, San Diego, CA) was dissolved in dimethyl sulfoxide and further diluted in saline (dimethyl sulfoxide 0.1%). The JAK2 inhibitor tyrphostin AG490 and the calcium ion chelator EGTA were from Calbiochem and Sigma Chemical, respectively. L-[^{3}H]arginine (1 mCi) was obtained form PerkinElmer Life Sciences, and cyclic guanosine monophosphate (cGMP) assay kits were from Cayman (Ann Arbor, MI).

Tissue extraction and immunoprecipitation. Rats were anesthetized with sodium thiopental (100 mg/kg body wt) and used 10–15 min later. As soon as anesthesia was assured by the loss of pedal and corneal reflexes, the thoracic cavity was open and the thoracic aorta was isolated and kept for 45 min at 37°C in Krebs-bicarbonate buffer equilibrated with 95% O_2:5% CO_2, pH 7.4, before being stimulated with insulin or ACh. It then was frozen with liquid N_2, powdered with a glass Dounce homogenizer on ice for at least 80 strokes, and immediately homogenized in extraction buffer, as described elsewhere (15). Extracts were centrifuged at 30,000*g* and 4°C for 45 min to remove insoluble material.

Protein analysis by immunoblotting. The precipitated proteins and/or whole-tissue extracts were treated with Laemmli sample buffer and then subjected to SDS-PAGE in a Bio-Rad miniature slab gel apparatus (Mini-Protean), as previously described (15,27).

JAK2 in vitro kinase activity assay. The protein kinase activity of the immunoprecipitates was measured as previously described (28).

Hyperinsulinemic-euglycemic clamp. After 5 h of fasting, six animals from each group were anesthetized intraperitoneally with sodium pentobarbital (50 mg/kg body wt), and catheters were then inserted into the left jugular vein (for glucose and insulin infusion) and carotid artery (for blood sampling), as previously described (29).

Blood pressure measurement. Blood pressure measurements in conscious rats were conducted by a tail-cuff system (MKIV; Narco BioSystems, Austin, TX) (30).

Vascular reactivity studies. In these studies, control and obese rats were anesthetized with halothane (Cristália Laboratories, Itapira, Brazil) and killed by decapitation. The chest of each rat was opened and the entire descending thoracic aorta was excised quickly. Tissues were prepared as previously described (31). After a 1-h stabilization period, the rings were precontracted with phenylephrine (1 μmol/l). Cumulative concentration-response curves to insulin, ACh, or glyceryl trinitrate (GTN) were obtained in intact aortic rings. Concentration-response curves to GTN also were constructed in endothelium-denuded aortic rings. In these rings, the endothelium was removed mechanically by rubbing the lumen of the aorta with a closed pair of fine-tipped forceps. The absence of the endothelium was confirmed by the loss of a relaxant response to ACh at the start of the experiments. Relaxations were plotted as percentages of the contraction induced by phenylephrine. In another experiment, aortic rings were incubated for 30 min with specific inhibitors AG490 (10 μmol/l) or LY294002 (50 μmol/l) before being stimulated with ACh in order to study the effects of the blockade of JAK2 or PI 3-kinase, respectively, over ACh-induced vascular relaxation.

L-[^{3}H]arginine to L-[^{3}H]citrulline conversion assay. Determination of eNOS catalytic activity in intact cells was performed by measuring of the conversion of L-[^{3}H]arginine to L-[^{3}H]citrulline as previously described (32). The cells were treated with ACh (10^{-5} mol/l) or insulin (10^{-7} mol/l) for 15 min, and in selected experiments cells were preincubated with LY294002 or AG490 for 30 min. Under all conditions, the L-[^{3}H]citrulline generation was fully inhibited by 2 mmol/l nitro-L-arginine methyl ester. In individual experiments, a minimum of three wells were used for each treatment group. All findings were confirmed in at least six independent studies.

Estimation of endothelium-derived NO. Confluent rabbit aortic endothelial cells in six-well plates were equilibrated for 30 min in physiological saline solution (PSS) supplemented with 250 μmol/l 3-isobutyl-1-methylxanthine and 250 μmol/l L-arginine in the absence or presence of nitro-L-arginine methyl ester or the inhibitor of interest (LY294002 or AG490). Equilibrated cells then were exposed to ACh (10^{-5} mol/l) or insulin (10^{-7} mol/l) for 30 min before the cells were lysed by the addition of 6% ice-cold trichloroacetic acid. Cell lysates then were subjected to centrifugation at 12,000*g* for 10 min, and determination of cGMP in supernatants was performed as described (33) in accordance with the kit assay.

Statistical analysis. Experiments were carried out by studying the groups of animals in parallel (animals fed a standard diet versus animals fed a high-fat diet). Data are means ± SE, accompanied by the indicated number of independent experiments. For comparisons, ANOVA was used. The significance level was set at P value <0.05. A statistics software was used (Instat v. 3.05; GraphPad).

RESULTS

Insulin signaling pathway in aorta of control animals. The presence of phosphorylated IRS-1 was detectable 5 min after incubation with insulin and was maximal at 15 min, and 30 min after incubation, IRS-1 tyrosine phosphorylation was nearly undetectable (Fig. 1*A*, *upper panel*). Nitrocellulose membranes of IRS-1 immunoprecipitates were stripped and reblotted with antibodies against p85 (PI 3-kinase), showing that the maximum level of association between these proteins occurred at 15 min (Fig. 1*A*, *middle panel*). Insulin also was able to stimulate JAK2 tyrosine phosphorylation 5 min after incubation with the hormone, reaching maximal levels at 15 min (Fig. 1*B*, *upper panel*). The association between JAK2 and IRS-1 also was investigated (Fig. 1*B*, *middle panel*), revealing the same temporal pattern of insulin-induced JAK2 tyrosine phosphorylation. Insulin treatment did not modulate the expression of IRS-1 and JAK2 (Fig. 1*A* and *B*, *lower panels*). Insulin-stimulated Akt serine phosphorylation was maximal 15 min after incubation with this hormone (Fig. 1*C*, *upper panel*), without any significant change in Akt protein levels (Fig. 1*C*, *lower panel*). Insulin led to an approximately four-fold increase above basal state in eNOS serine phosphorylation at 15 min (Fig. 1*D*, *upper panel*), without significant changes in eNOS tissue levels (Fig. 1*D*, *lower panel*). It also was observed that insulin was able to stimulate the phosphorylation of ERK1/2 isoforms of

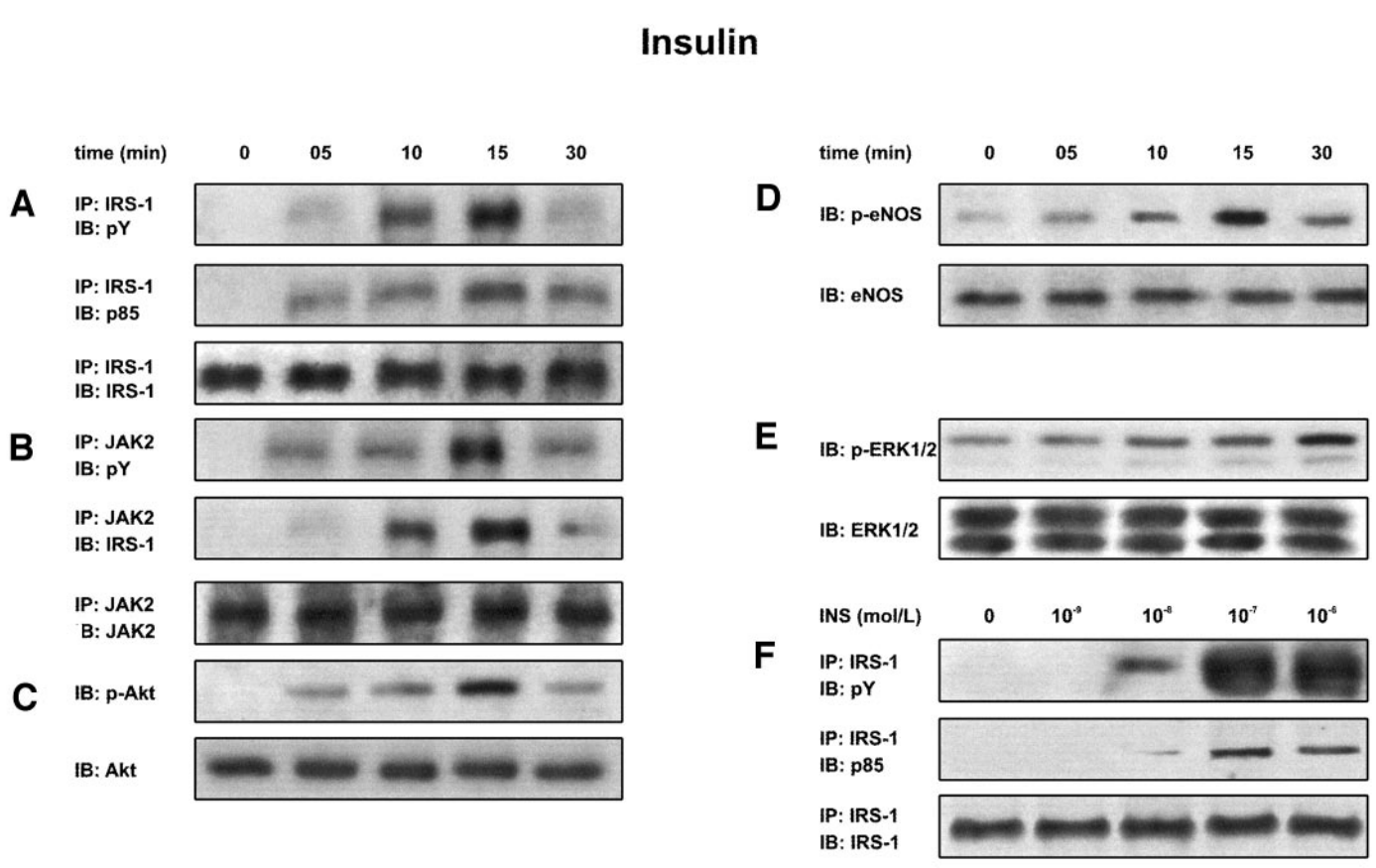

FIG. 1. Insulin signaling in aorta of control rats (time and dose response). Aortae were incubated with medium with or without insulin, frozen, and powdered as described in RESEARCH DESIGN AND METHODS, and extracts were submitted to immunoprecipitation (IP) followed by immunoblotting (IB). *A*: Immunoprecipitation with α-IRS-1 and immunoblotting with α-pY (*upper panel*); immunoprecipitation with α-IRS-1 and immunoblotting with α-p85 (*middle panel*); immunoprecipitation with α-IRS-1 and immunoblotting with α-IRS-1 (*lower panel*). *B*: Immunoprecipitation with α-JAK2 and immunoblotting with α-pY (*upper panel*); immunoprecipitation with α-JAK2 and immunoblotting with α-IRS-1 (*middle panel*); immunoprecipitation with α-JAK2 and immunoblotting with α-JAK2 (*lower panel*). *C*: Immunoblotting with α-p-Akt (*upper panel*); immunoblotting with α-Akt (*lower panel*). *D*: Immunoblotting with α-p-eNOS (*upper panel*); immunoblotting with α-eNOS (*lower panel*). *E*: Immunoblotting with α-p-ERK1/2 (*upper panel*); immunoblotting with α-ERK1/2 (*lower panel*). *F*: Immunoprecipitation with α-IRS-1 and immunoblotting with α-pY (*upper panel*); immunoprecipitation with α-IRS-1 and immunoblotting with α-p85 (*middle panel*); immunoprecipitation with α-IRS-1 and immunoblotting with α-IRS-1 (*lower panel*). Blots are representative of six independent experiments each.

MAPK, leading them to a maximum activation by 15–30 min (Fig. 1*E*, *upper panel*), without any significant change in protein levels (Fig. 1*E*, *lower panel*). Insulin-stimulated IRS-1 tyrosine phosphorylation, as well as its association with p85 subunit, was dose dependent; they both were detectable after incubation with 10^{-8} mol/l insulin. Maximal effect occurred at 10^{-7} mol/l (Fig. 1*F*).

ACh signaling pathway in aorta of control animals. ACh induces JAK2 tyrosine phosphorylation 5 min after incubation with this hormone, reaching maximum levels by 15 min (Fig. 2*A*, *upper panel*). Next, the association between JAK2 and IRS-1 was evaluated, being maximal at 15 min (Fig. 2*A*, *middle panel*). The tissue levels of JAK2 did not change among the samples (Fig. 2*A*, *lower panel*). ACh also was able to stimulate the tyrosine phosphorylation of IRS-1, as well as its association with PI 3-kinase, in a time-dependent manner (Fig. 2*B*, *upper* and *middle panels*), without changes in IRS-1 protein expression (Fig. 2*C*, *lower panel*). To test whether JAK2 kinase activity could be stimulated by ACh in rat aorta, we measured the enzyme autophosphorylation in vitro by immunoprecipitating aorta extracts (with or without a low concentration of ACh) with α-JAK2 and performed an in vitro kinase assay using ATP, as described above. JAK2 kinase activity was increased significantly in aorta extracts after incubation with ACh for 15 min, as demonstrated by an increase in JAK2 autophosphorylation (Fig. 2*C*). ACh also stimulated Akt ser473 phosphorylation maximally after 15 min (Fig. 2*D*, *upper panel*), without any change in Akt protein levels (Fig. 2*D*, *lower panel*). ACh resulted in an approximately fivefold increase in eNOS serine phosphorylation above basal at 15 min (Fig. 2*E*, *upper panel*), without changes in eNOS tissue levels (Fig. 2*E*, *lower panel*). ACh also stimulated the phosphorylation of ERK1/2, leading them to a maximum activation by 15–30 min (Fig. 2*F*, *upper panel*), without any modulation in their protein levels (Fig. 2*F*, *lower panel*). ACh-stimulated IRS-1 tyrosine phosphorylation, as well as its association with p85 subunit, was dose dependent; they both were detectable after the incubation with 10^{-5} mol/l and were maximal with 10^{-4} mol/l, decreasing to ~60% of the maximum with 10^{-3} mol/l ACh (Fig. 2*G*). Similar results were obtained in tissue extracts immunoprecipitated with anti-JAK2 followed by immunoblotting with anti-phosphotyrosine antibodies (Fig. 2*G*, *lower panel*).

Effects of blockade of proximal activators of eNOS. To evaluate the importance of JAK2 or PI 3-kinase over the activation of eNOS, we conducted controlled experiments

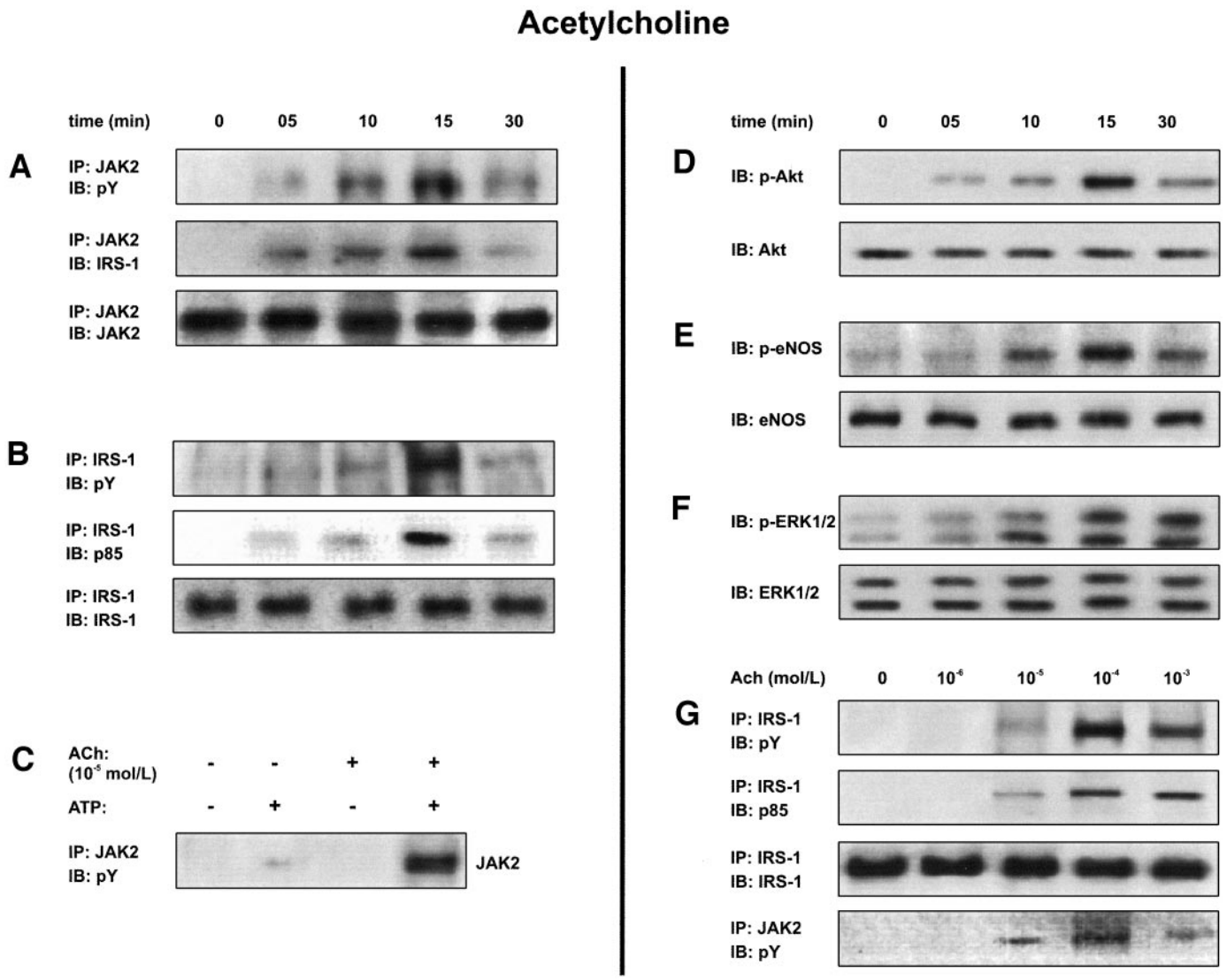

FIG. 2. ACh signaling in aorta of control rats (time and dose response). Aortae were incubated with medium with or without ACh, frozen, and powdered as described in RESEARCH DESIGN AND METHODS, and extracts were submitted to immunoprecipitation (IP) followed by immunoblotting (IB). *A*: Immunoprecipitation with α-JAK2 and immunoblotting with α-pY (*upper panel*); immunoprecipitation with α-JAK2 and immunoblotting with α-IRS-1 (*middle panel*); immunoprecipitation with α-JAK2 and immunoblotting with α-JAK2 (*lower panel*). *B*: Immunoprecipitation with α-IRS-1 and immunoblotting with α-pY (*upper panel*); immunoprecipitation with α-IRS-1 and immunoblotting with α-p85 (*middle panel*); immunoprecipitation with α-IRS-1 and immunoblotting with α-IRS-1 (*lower panel*). *C*: JAK2 tyrosine activity measured by autophosphorylation in vitro. Thoracic aortae were incubated with (+) or without (−) a very low concentration of ACh (10^{-5} mol/l) and used 15 min later (maximum JAK2 tyrosine phosphorylation in aorta) to stimulate partial JAK2 autophosphorylation. JAK2 was immunoprecipitated (2 μg/ml) and allowed to autophosphorylate in vitro in the presence (+) or absence (−) of exogenous ATP. Tyrosine phosphorylation was measured by immunoblotting with αPY (1 μg/ml). *D*: Immunoblotting with α-p-Akt (*upper panel*); immunoblotting with α-Akt (*lower panel*). *E*: Immunoblotting with α-p-eNOS (*upper panel*); immunoblotting with α-eNOS (*lower panel*). *F*: Immunoblotting with α-p-ERK1/2 (*upper panel*); immunoblotting with α-ERK1/2 (*lower panel*). *G*: Immunoprecipitation with α-IRS-1 and immunoblotting with α-pY (*upper panel*); immunoprecipitation with α-IRS-1 and immunoblotting with α-p85 (*middle panel*); immunoprecipitation with α-IRS-1 and immunoblotting with α-IRS-1 (*lower panel*); immunoprecipitation with α-JAK2 and immunoblotting with α-pY (*lowest panel*). Blots are representative of six independent experiments each.

in aortic tissue with the aid of specific pharmacological inhibitors AG490 or LY294002, respectively (Fig. 3*A*). ACh-stimulated IRS-1 tyrosine phosphorylation was not affected by the presence of LY294002, but it was almost completely abolished when aortae were preincubated with AG490 (Fig. 3*A*, *upper panel*). The presence of AG490, as expected, completely inhibited ACh-stimulated tyrosine phosphorylation of JAK2, whereas LY294002 had no effect on this event (Fig. 3*A*, *next panel*). Treatment of aortae with AG490 or LY294002 abolished ACh-induced Akt and ERK1/2 phosphorylation but only reduced eNOS phosphorylation, suggesting that eNOS can be partially activated by a pathway independent of JAK2/IRS-1/Akt (Fig. 3*A*, *lower panels*).

The endothelial function then was evaluated by the endothelial-dependent vasorelaxation in response to ACh in the presence or absence of AG490 or LY294002 (Fig. 3*B*). The potency of ACh (pEC_{50}: 6.85 ± 0.01, $n = 5$) was significantly reduced in the presence of AG490 (pEC_{50}: 6.36 ± 0.09, $n = 7$, $P < 0.01$) or LY294002 (pEC_{50}: 5.97 ± 0.20, $n = 6$, $P < 0.01$). Similarly, the maximal responses produced by ACh (86 ± 2%, $n = 5$) were significantly inhibited after incubation with AG490 (64 ± 6%, $n = 7$, $P \leq 0.05$) or LY294002 (44 ± 3%, $n = 6$, $P < 0.001$).

Because more than one cell type comprises the isolated aorta, next we conducted experiments in cultured aortic endothelial cells. Also, in order to evaluate the relative participation of calcium-dependent and -independent path-

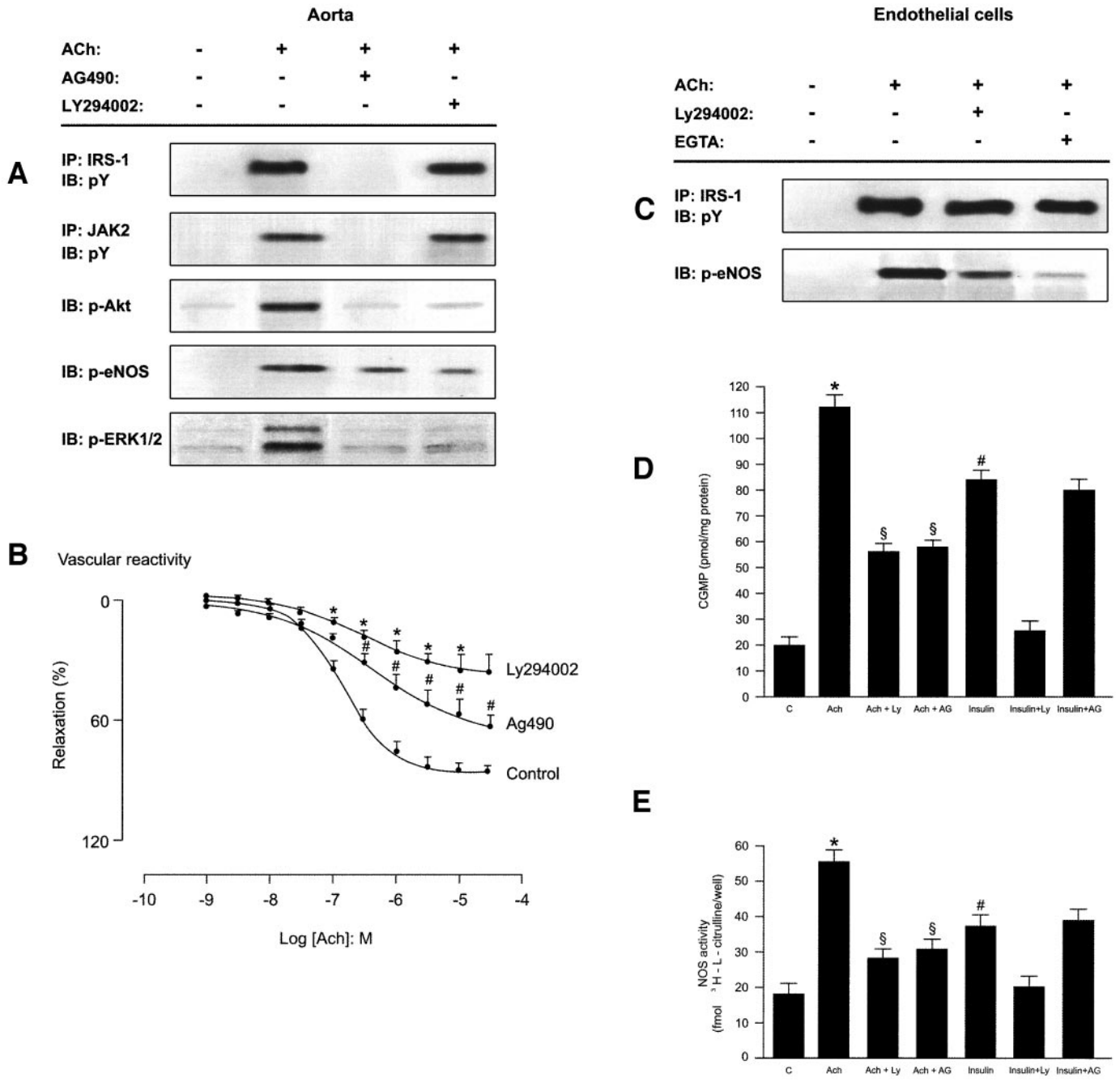

FIG. 3. Effects of pharmacological inhibitors on ACh signaling and vascular reactivity in aortae and on ACh-stimulated eNOS phosphorylation and NOS actitivy in endothelial cells. *A*: Fresh aortae were incubated with medium with or without ACh (10^{-4} mol/l) and specific pharmacological inhibitors (50 μmol/l LY294002 or 10 μmol/l AG490), frozen, and powdered as described in RESEARCH DESIGN AND METHODS, and extracts were submitted to immunoprecipitation (IP) followed by immunoblotting (IB). Immunoprecipitation with α-IRS-1 and immunoblotting with α-pY (*upper panel*); immunoprecipitation with α-JAK2 and immunoblotting with α-pY (*middle panel*); immunoblotting with α-p-Akt (*middle panel*); immunoblotting with α-p-eNOS (*middle panel*) and immunoblotting with α-p-ERK1/2 (*lower panel*). *B*: Vascular reactivity in the aortic rings of control rats preincubated with 50 μmol/l LY294002 or 90 μmol/l AG4. Experimental values were calculated relative to the maximal changes from the contraction produced by phenylephrine in each tissue, which was taken as 100%. The pEC_{50} values for ACh were determined as −log of the molar concentration to produce 50% of the maximal relaxation in phenylephrine-contracted tissues. *C*: Rabbit endothelial cells (REC) were incubated with medium with or without ACh (10^{-4} mol/l) and specific pharmacological inhibitors (50 μmol/l LY294002 or 5 μmol/l EGTA) and were homogenized, and extracts were submitted to immunoprecipitation (IP) followed by immunoblotting (IB). Immunoprecipitation with α-IRS-1 and immunoblotting with α-pY (*upper panel*); immunoblotting with α-p-eNOS (*lower panel*). Intact cells (REC) were pretreated with vehicle, LY294002 or AG490, for 30 min and then stimulated with insulin or ACh for 15 min, and the L-[^{3}H]arginine conversion to L-[^{3}H]citrulline was assessed (*D*). REC were pretreated with the same blockers and then incubated with insulin or ACh for 30 min, and cGMP accumulation was determined (*E*). Data are shown as the percentage of relaxation of six independent experiments, expressed as means ± SE. **P* < 0.001 treated vs. control; #*P* < 0.05 treated vs. control; §*P* < 0.05 ACh vs. ACh plus inhibitors.

ways by which ACh can activate eNOS, we incubated endothelial cells with EGTA (a specific intracellular calcium ion chelator) or LY294002 (Fig. 3*C*). The ACh-stimulated tyrosine phosphorylation of IRS-1 was not affected by any of these two inhibitors (Fig. 3*C*, *upper panel*). Treatment of endothelial cells with any of these inhibitors, however, reduced the activation of eNOS by different degrees: LY294002 reduced ACh stimulation of

TABLE 1
Metabolic and biochemical characteristics of the experimental animals

	Control	Obese
Body weight (g)	270 ± 20 (10)	350 ± 30 (10)*
Bilateral epididymal fat (g/100 g)	2.21 ± 0.20 (10)	3.68 ± 0.32 (10)*
Bilateral perirenal fat (g/100 g)	2.34 ± 0.09 (10)	2.98 ± 0.15 (10)*
Mesenteric fat (g/100 g)	3.08 ± 0.40 (10)	5.50 ± 0.50 (10)*
Blood glucose (mmol/l)	5.72 ± 0.9 (10)	6.00 ± 0.4 (10)
Serum insulin (pmol/l)	10.2 ± 1.1 (10)	21.5 ± 2.6 (10)*
Serum triglycerides (mmol/l)	0.56 ± 0.09 (10)	1.61 ± 0.13 (10)†
Serum cholesterol (mmol/l)	1.55 ± 0.13 (10)	1.65 ± 0.10 (10)
Serum HDL (mg/dl)	1.16 ± 0.11 (10)	1.08 ± 0.07 (10)
Glucose infusion rates ($mg \cdot kg^{-1} \cdot min^{-1}$)	23 ± 4 (6)	8 ± 2 (6)*
Systolic blood pressure (mmHg)	110 ± 2 (10)	114 ± 4 (10)

Data are means ± SE (n). Steady-state glucose infusion rates were obtained from averaged rates of 90–120 min of 10% glucose infusion during hyperinsulinemic-euglycemic clamp procedures. *$P < 0.01$ vs. control; †$P < 0.0001$ vs. control.

eNOS serine phosphorylation to ~60% of controls, and a greater inhibition (to ~30% of controls) of eNOS was observed when cells were treated with EGTA before being stimulated with ACh (Fig. 3*C*, *lower panel*).

We also investigated in endothelial cells the effects of LY294002 and aG490 on ACh or insulin-induced NOS activity, by the L-[^{3}H]arginine conversion to L-[^{3}H]citrulline and on endothelial NO production by the increase in cellular cGMP content. The results showed that ACh had the stronger ability to induce NOS activation and cGMP accumulation, and this effect was reduced by ~50% when the cells are pretreated with LY or AG490 (Fig. 3*D* and *E*). Insulin also increased NOS activity and cGMP accumulation, but this effect was weaker than ACh. Treatment of cells for 30 min with LY294002 completely blocked insulin's effect on cGMP accumulation. However, treatment of these cells with AG490 for 30 min had no effect on the ability of insulin to activate NOS and induce NO production (Fig. 3*D* and *E*).

PI 3-kinase and MAPK pathways in aorta of obese animals: effect of insulin and ACh. The effect of obesity on ACh-induced IRS-1/PI 3-kinase/Akt/eNOS activation as well as on ERK1/2 MAPK isoforms was studied in male Wistar rats fed a high-fat diet for 60 days. Characteristics of these animals are detailed in Table 1. Animals fed a high-fat diet for 60 days were significantly heavier than those fed a standard rodent diet and presented higher contents of visceral adipose tissue in different sites, were also more insulin resistant, and had higher fasting insulin and triacylglycerol levels than controls. Systolic blood pressure was normal and similar in both groups of animals.

Obese rats presented endothelial dysfunction, with significant reductions in endothelial-dependent vasorelaxation in response to both ACh and insulin (Fig. 4) when compared with their age-matched controls. ACh produced a concentration-dependent relaxation in endothelium-intact preparations with a pEC_{50} value of 6.85 ± 0.02, whereas in obese rats there was a significant reduction in the pEC_{50} value (6.59 ± 0.01, $P < 0.001$). Furthermore,

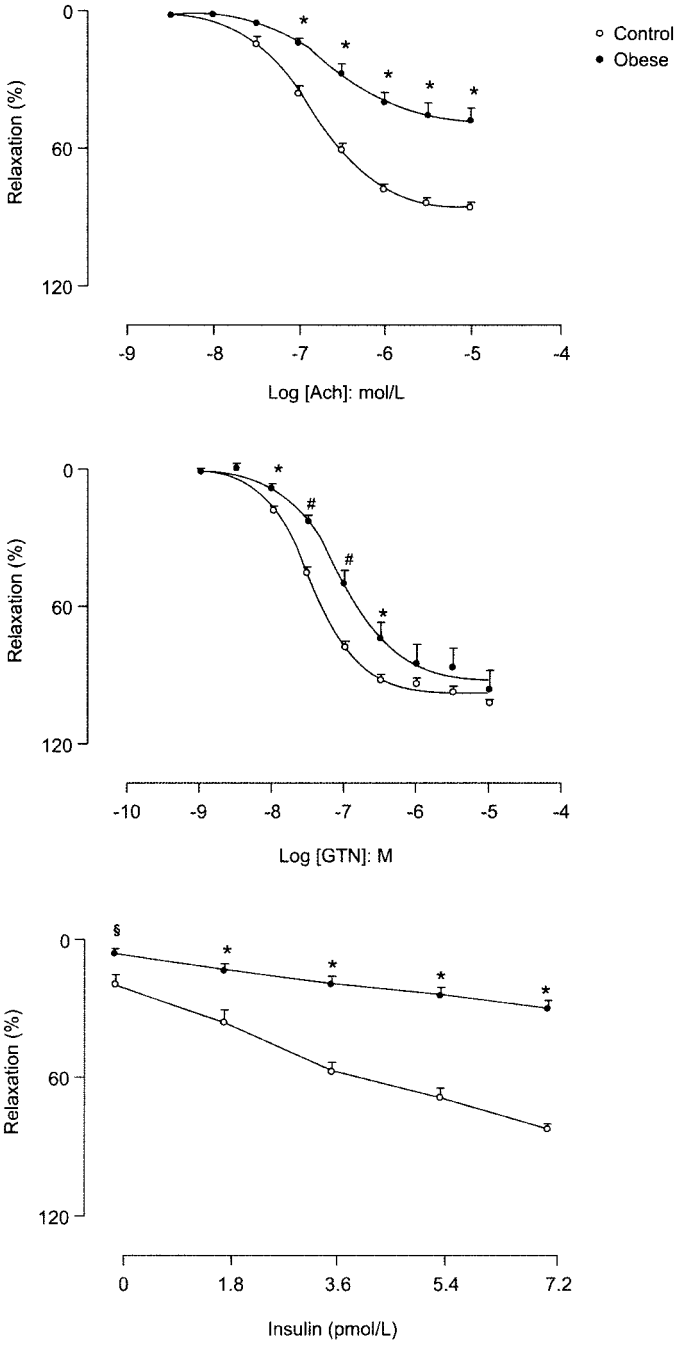

FIG. 4. Vascular reactivity in the aortic rings. Experimental values were calculated relative to the maximal changes from the contraction produced by phenylephrine in each tissue, which was taken as 100%. The pEC_{50} values for ACh and GTN were determined as −log of the molar concentration to produce 50% of the maximal relaxation in phenylephrine-contracted tissues. Data are shown as the percentage of relaxation of six independent experiments, expressed as means ± SE. *$P < 0.001$; #$P < 0.01$; §$P < 0.05$ obese vs. control.

ACh-induced maximum relaxation was attenuated by 44% in obese rats (86 ± 2 and 48 ± 5%, control vs. obese, respectively; $P < 0.001$), whereas the relaxations elicited by insulin were reduced by ~66% at all concentrations assayed. The potency of the endothelium-independent relaxation produced by GTN also was reduced in intact aortic rings of obese rats (pEC_{50}: 7.45 ± 0.04 vs. 7.06 ± 0.04, control vs. obese, respectively; $P < 0.001$). However, after endothelium denudation, the potency of GTN was potentiated in both groups (pEC_{50}: 7.75 ± 0.01 and 7.82 ±

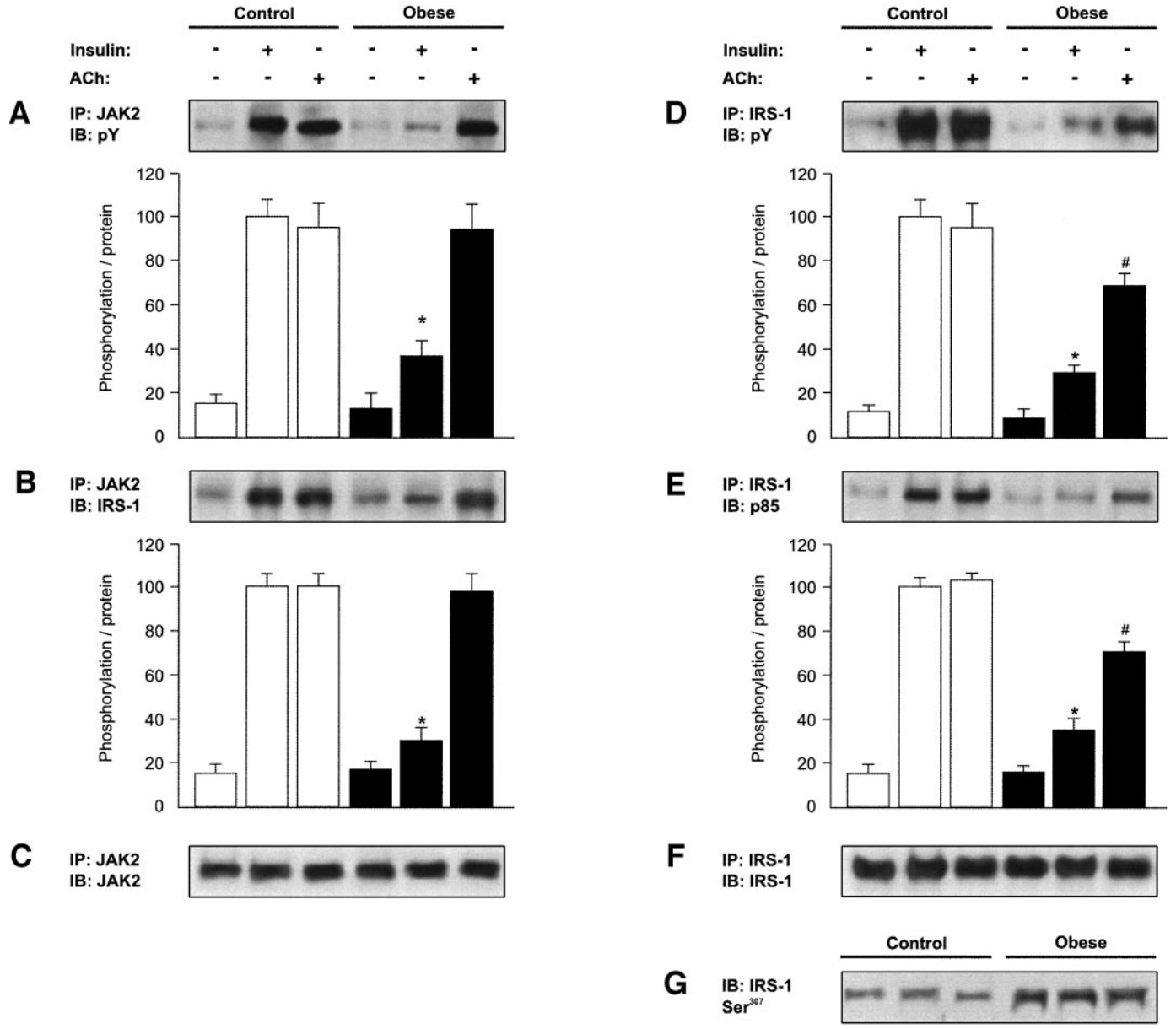

FIG. 5. Insulin signaling in aorta of control and obese rats. Aortae were incubated with medium with or without insulin (10^{-7} mol/l) or ACh (10^{-4} mol/l), frozen, and powdered as described in RESEARCH DESIGN AND METHODS, and extracts were submitted to immunoprecipitation (IP) followed by immunoblotting (IB). *A*: Immunoprecipitation with α-JAK2 and immunoblotting with α-pY. *B*: Immunoprecipitation with α-JAK2 and immunoblotting with α-IRS-1. *C*: Immunoprecipitation with α-JAK2 and immunoblotting with α-JAK2. *D*: Immunoprecipitation with α-IRS-1 and immunoblotting with α-pY. *E*: Immunoprecipitation with α-IRS-1 and immunoblotting with α-p85. *F*: Immunoprecipitation with α-IRS-1 and immunoblotting with α-IRS-1. *G*: Basal IRS-1^{ser307} phosphorylation (immunoblotting with α-IRS-1^{ser307}). The results of scanning densitometry are shown and indicate arbitrary units relative to phosphorylation (or association)/protein level. Values are means ± SE of six independent experiments each. *P < 0.001, insulin-stimulated obese vs. insulin-stimulated control; #P < 0.001, ACh-stimulated obese vs. ACh-stimulated control.

0.01, control vs. obese, respectively; data not shown). It has been reported that the endothelium-independent relaxations induced by NO donors are potentiated in eNOS knockout mice (34) or not affected after endothelium denudation in rats (35). Our results demonstrate a significant decrease in the potency of GTN in endothelium-intact aorta of obese rats. Nevertheless, it does not involve changes in the vascular smooth muscle cells because the relaxation produced by GTN was potentiated in both control and obese groups after mechanic endothelium denudation. Taken together, these data suggest that the impaired relaxations observed herein are related to an endothelial dysfunction.

Insulin-stimulated JAK2 tyrosine phosphorylation was significantly reduced (~60%) in aortae from obese animals when compared with controls, but there was no difference in JAK2 phosphorylation when tissues were incubated with ACh (Fig. 5*A*). Moreover, the association between JAK2 and IRS-1 in aortae from obese rats also was significantly reduced when vessels were incubated with insulin but not with ACh (Fig. 5*B*). Tissue levels of JAK2 did not vary between the two groups of animals (Fig. 5*C*). There was a great decrease (~70%) in insulin-stimulated IRS-1 tyrosine phosphorylation in aorta from obese animals when compared with controls (Fig. 5*D*). ACh-stimulated IRS-1 tyrosine phosphorylation also was reduced

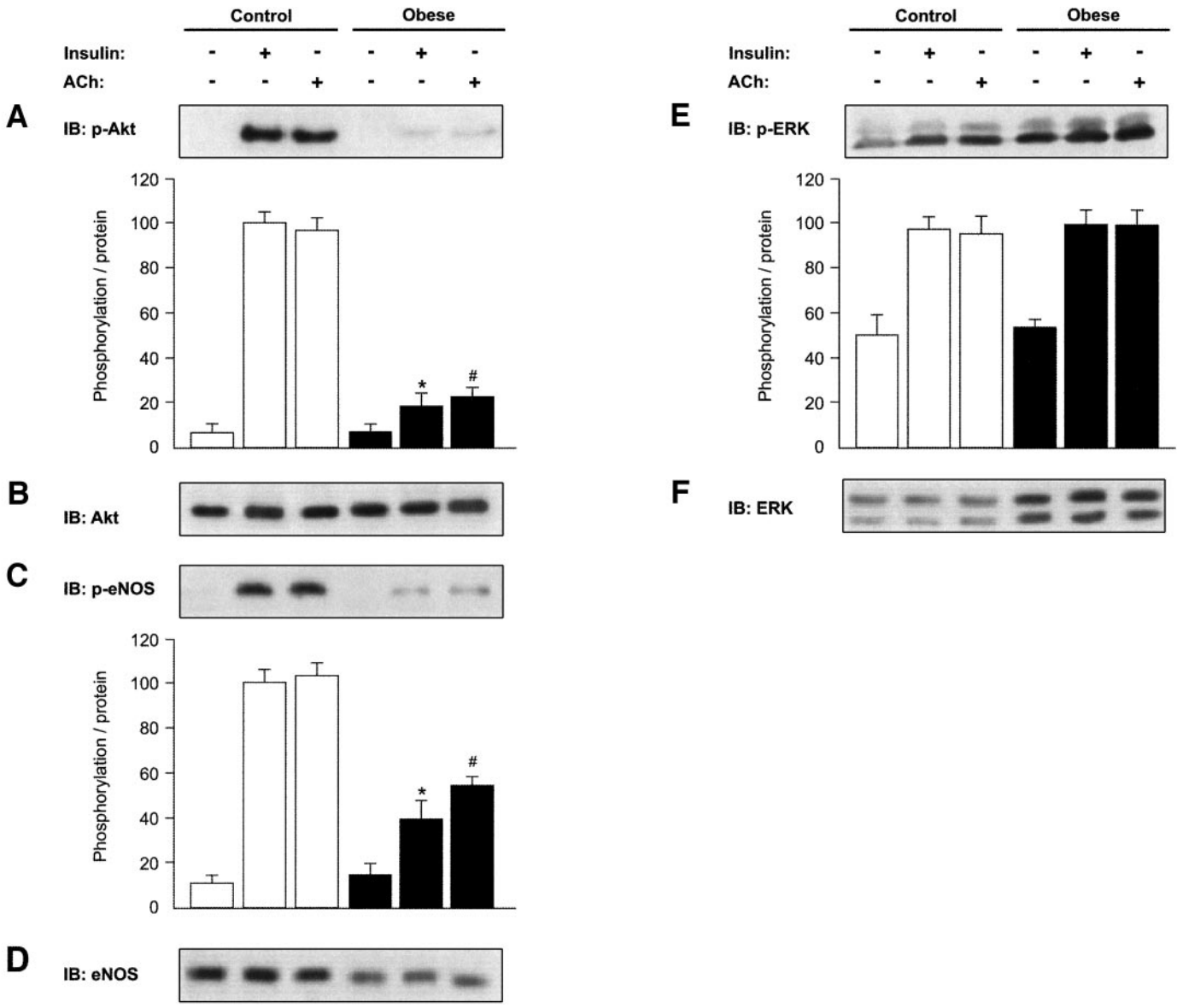

FIG. 6. Insulin signaling in aortae of control and obese rats. Aortae were incubated with medium with or without insulin (10^{-7} mol/l) or ACh (10^{-4} mol/l), frozen, and powdered as described in RESEARCH DESIGN AND METHODS, and extracts were submitted to immunoprecipitation (IP) followed by immunoblotting (IB). *A*: Immunoblotting with α-p-Akt. *B*: Immunoblotting with α-Akt. *C*: Immunoblotting with α-p-eNOS. *D*: Immunoblotting with α-eNOS. *E*: Immunoblotting with α-p-ERK1/2. *F*: Immunoblotting with α-ERK1/2. The results of scanning densitometry are shown and indicate arbitrary units relative to phosphorylation/protein level. Values are means ± SE of six independent experiments each. **P* < 0.001, insulin-stimulated obese vs. insulin-stimulated control; #*P* < 0.001, ACh-stimulated obese vs. ACh-stimulated control.

(~30%) in aortae from obese animals compared with controls (Fig. 5*D*). The insulin- and ACh-stimulated association between IRS-1 and the p85 regulatory subunit of PI 3-kinase both were diminished in aortae from obese rats compared with their controls (Fig. 5*E*). There was no significant difference between the protein concentrations of IRS-1 in aortae from both groups of animals (Fig. 5*F*). Obese animals presented significantly higher basal contents of IRS-1^{ser307} phosphorylation (~2.5-fold higher) in their aortae when compared with control animals (Fig. 5*G*). Obese rats showed reduced Akt activation after insulin and ACh stimulus (~80%) compared with controls (Fig. 6*A*), with no differences between the protein concentrations of Akt in aortae from these two groups (Fig. 6*B*). The serine phosphorylation of eNOS in aortae from obese rats was significantly reduced in both response to insulin (by ~70%) and also to ACh (by ~60%) (Fig. 6*C*) when compared with controls. eNOS tissue levels in aortae from obese rats was significantly reduced by ~30% compared with controls (Fig. 6*D*). In addition, the ratio of phosphorylation per protein of eNOS also was reduced in obese rats after stimulation with insulin (by ~60%) and ACh (by ~40%). Obese rats showed increased basal tyrosine phosphorylation of ERK1/2, 2.3-fold higher than those found in controls ($P < 0.001$; Fig. 6*E*). After incubation with insulin or ACh, tyrosine phosphorylation of ERK1/2 was 1.7 and 1.6 times higher, respectively, in aortae from obese rats than in the control rats ($P < 0.001$; Fig. 6*E*). However, obese rats demonstrated ~2.0 times higher protein levels of ERK1/2 in aortae than the control rats ($P < 0.001$; Fig. 6*F*), suggesting that increased ERK1/2 tyrosine phosphorylation was attributed to increased levels of these kinases found in aortae of obese animals.

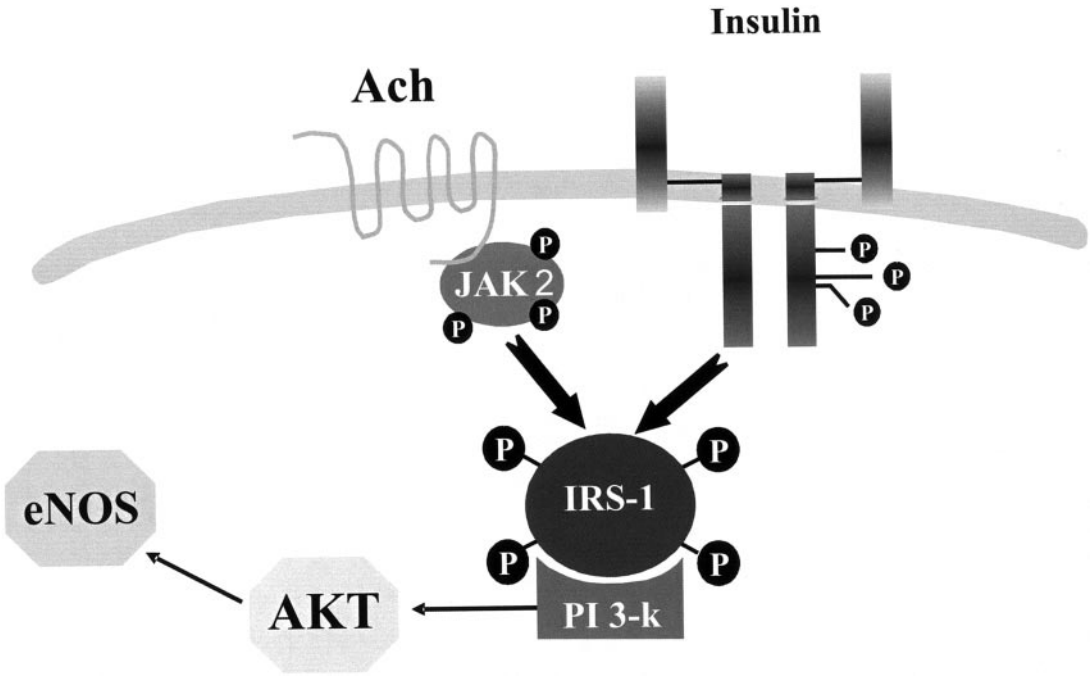

FIG. 7. Alternative pathway through JAK2/IRS-1/PI 3-kinase/AKT by which ACh can induce eNOS activation.

DISCUSSION

Here, we show that ACh can activate eNOS through the IRS-1/PI 3-kinase/Akt pathway in rat aorta and in endothelial cells. Also, we show that in an animal model of insulin resistance and obesity (i.e., rats fed a high-fat diet for 60 days), ACh and insulin signaling through this pathway in aorta is blunted. This study provides data to the hypothesis that the endothelial dysfunction in aorta of obese rats is related to insulin and ACh resistance.

The results of the present study show that ACh activates the JAK2/IRS-1 signaling pathway, as described by others' G-protein–coupled receptors (36,37), and by inducing IRS-1 tyrosine phosphorylation, is able to activate the PI 3-kinase/Akt/eNOS pathway (Fig. 7), suggesting another pathway by which ACh can induce eNOS activation. The pharmacological blockade of JAK2 or PI 3-kinase was able to reduce ACh-stimulated eNOS activation/phosphorylation and cGMP accumulation by ~50%, suggesting that this pathway may have an important role in ACh-induced eNOS activity but certainly is not the only pathway that accounts for this ACh effect. Although insulin also activated JAK2 tyrosine phosphorylation, the pharmacological blockade of JAK2 did not change insulin-induced IRS-1 tyrosine phosphorylation or Akt phosphorylation in neither insulin effect nor on eNOS activity and aorta relaxation, suggesting that JAK2 is not necessary for the insulin action in aorta. Thus, the requirement for insulin to activate IRS system via JAK2 seems redundant, and it is corroborated by a recent study (38) in transfected L6 myotubes with siRNA against JAK2. As expected, the effect of ACh in causing eNOS activation, cGMP accumulation, and endothelial-dependent vasorelaxation is stronger than insulin.

Tyrosine-phosphorylated IRS-1 also can proceed through the Grb2/SOS and Ras pathway, leading to the activation of ERK1 and 2 (39). The present study demonstrates that ACh induces ERK/MAPK activation and that JAK2 has an important role in this activation. Furthermore, the present results are in accordance with recent evidence that ACh activates ERK/MAPK (40,41).

Our results showed impaired relaxation of the aorta induced by insulin or ACh in obese rats as a consequence of endothelial dysfunction. These animals represent a very adequate model of metabolic syndrome, characterized by insulin resistance, central fat depot, increase in triacylglycerol levels, and cardiovascular disease demonstrated by endothelial dysfunction. We did not observe hypertension in these animals. Hypertension is not always uniformly observed in diet-induced obesity or in other animal models of insulin resistance with endothelial dysfunction (42,43). It is possible that the rat strain, and mainly the duration of the diet, may influence the development of hypertension. Recently, it was demonstrated that insulin resistance and endothelial dysfunction precedes the development of hypertension, and in some strains it might take ≥1 year of high-fat diet to induce hypertension (43,44).

The expression of eNOS apparently is regulated by the insulin receptor–mediated PI 3-kinase signaling pathway (6). Selective inhibition of insulin actions on the PI 3-kinase pathway in vasculature in insulin-resistant states, with preservation of Ras/Raf/MEK/ERK pathway, has been proposed as an important cause of NO production downregulation, leading to an imbalance that could lead to the development of atherosclerosis (14,15). Although there was a reduction in insulin- and ACh-induced IRS-1 tyrosine phosphorylation, the activation of ERK1/2 by both hormones was increased in aorta of obese rats. This is because of the increase in ERK1/2 protein expression and probably also because other substrates of insulin receptors and JAK2, such as Shc, may compensate IRS-1 on ERK1/2 activation, as we demonstrated in aorta of another animal model of insulin resistance, the spontaneously hypertensive rat (15).

It has been reported that in states of insulin resistance and obesity, activation of some serine kinases induces ser307 phosphorylation of IRS-1 (45,46), leading to a decrease in insulin-stimulated PI 3-kinase activity. The reduction in insulin-stimulated IRS-1 tyrosine phosphorylation was associated with an increase in IRS-1 ser307

phosphorylation in aorta of obese animals. The negative modulation of IRS-1 could make this substrate more refractory to the activation by insulin as well as by ACh. The ACh-stimulated activation of JAK2 is not altered in obese rats when compared with controls. However, the activation of eNOS was reduced in response to both insulin and ACh in obese rats. The reduced activation of eNOS in aorta of obese rats could be due to reduced stimulus through the IRS-1/PI 3-kinase/Akt pathway. Furthermore, this pathway also may have a role in the control of eNOS expression, and reduced signaling through IRS-1/PI 3-kinase/Akt may contribute to explain the lower eNOS levels in aorta of obese rats. Our data suggest that reduced eNOS expression and/or activation may have an important role in endothelial dysfunction of this obese animal. Important evidence that the IRS-1/PI 3-kinase pathway may be relevant for ACh signaling comes from mice lacking IRS-1 (47). In these animals, the relaxation induced by ACh was significantly reduced in aortic strips of IRS-1 knockout mice compared with controls. Taken together, given these previous results and the data presented herein, it can be suggested that the inhibition of IRS-1 function could represent a unifying mechanistic link between different factors involved in not only insulin resistance but also in endothelial dysfunction.

In summary, here we have documented a novel pathway of ACh-stimulated activation of eNOS, involving the JAK2/IRS-1/PI 3-kinase/Akt pathway. Aside from a normal activation of JAK2 in response to ACh in aorta of obese insulin-resistant rats, the increased IRS-1 ser307 content could inhibit the ability of IRS-1 to be activated by both insulin and ACh, leading to a reduction in the PI 3-kinase pathway activation and to a reduced expression of eNOS, producing endothelial dysfunction. These results suggest that in aorta of obese rats, there is not only insulin resistance but also ACh resistance, probably mediated by a common signaling pathway that controls the activity and the protein levels of eNOS.

ACKNOWLEDGMENTS

H.G.Z. holds a graduate fellowship from CAPES.

We thank Eszter DiMarzio, Luis Janieri, Márcio da Cruz, and Jósimo Pinheiro for their technical assistance.

REFERENCES

1. King GL, Goodman AD, Buzney S, Moses A, Kahn CR: Receptors and growth-promoting effects of insulin and insulinlike growth factors on cells from bovine retinal capillaries and aorta. *J Clin Invest* 75:1028–1036, 1985
2. Obata T, Kashiwagi A, Maegawa H, Nishio Y, Ugi S, Hidaka H, Kikkawa R: Insulin signaling and its regulation of system A amino acid uptake in cultured rat vascular smooth muscle cells. *Circ Res* 79:1167–1176, 1996
3. Zeng G, Quon MJ: Insulin-stimulated production of nitric oxide is inhibited by wortmannin: direct measurement in vascular endothelial cells. *J Clin Invest* 98:894–898, 1996
4. Anderson PW, Zhang XY, Tian J, Correale JD, Xi XP, Yang D, Graf K, Law RE, Hsueh WA: Insulin and angiotensin II are additive in stimulating TGF-beta 1 and matrix mRNAs in mesangial cells. *Kidney Int* 50:745–753, 1996
5. Tamaroglio TA, Lo CS: Regulation of fibronectin by insulin-like growth factor-I in cultured rat thoracic aortic smooth muscle cells and glomerular mesangial cells. *Exp Cell Res* 215:338–346, 1994
6. Kuboki K, Jiang ZY, Takahara N, Ha SW, Igarashi M, Yamauchi T, Feener EP, Herbert TP, Rhodes CJ, King GL: Regulation of endothelial constitutive nitric oxide synthase gene expression in endothelial cells and in vivo: a specific vascular action of insulin. *Circulation* 101:676–681, 2000
7. Papapetropoulos A, Rudic RD, Sessa WC: Molecular control of nitric oxide synthases in the cardiovascular system. *Cardiovasc Res* 43:509–520, 1999
8. Saltiel AR, Kahn CR: Insulin signalling and the regulation of glucose and lipid metabolism. *Nature* 414:799–806, 2001
9. Virkamaki A, Ueki K, Kahn CR: Protein-protein interaction in insulin signaling and the molecular mechanisms of insulin resistance. *J Clin Invest* 103:931–943, 1999
10. Dimmeler S, Fleming I, Fisslthaler B, Hermann C, Busse R, Zeiher AM: Activation of nitric oxide synthase in endothelial cells by Akt-dependent phosphorylation. *Nature* 399:601–605, 1999
11. Fulton D, Gratton JP, McCabe TJ, Fontana J, Fujio Y, Walsh K, Franke TF, Papapetropoulos A, Sessa WC: Regulation of endothelium-derived nitric oxide production by the protein kinase Akt. *Nature* 399:597–601, 1999
12. Sasaoka T, Ishiki M, Sawa T, Ishihara H, Takata Y, Imamura T, Usui I, Olefsky JM, Kobayashi M: Comparison of the insulin and insulin-like growth factor 1 mitogenic intracellular signaling pathways. *Endocrinology* 137:4427–4434, 1996
13. Sasaoka T, Rose DW, Jhun BH, Saltiel AR, Draznin B, Olefsky JM: Evidence for a functional role of Shc proteins in mitogenic signaling induced by insulin, insulin-like growth factor-1, and epidermal growth factor. *J Biol Chem* 269:13689–13694, 1994
14. Jiang ZY, Lin YW, Clemont A, Feener EP, Hein KD, Igarashi M, Yamauchi T, White MF, King GL: Characterization of selective resistance to insulin signaling in the vasculature of obese Zucker (fa/fa) rats. *J Clin Invest* 104:447–457, 1999
15. Zecchin HG, Bezerra RM, Carvalheira JB, Carvalho-Filho MA, Metze K, Franchini KG, Saad MJ: Insulin signalling pathways in aorta and muscle from two animal models of insulin resistance: the obese middle-aged and the spontaneously hypertensive rats. *Diabetologia* 46:479–491, 2003
16. Stuehr DJ: Structure-function aspects in the nitric oxide synthases. *Annu Rev Pharmacol Toxicol* 37:339–359, 1997
17. Gratton JP, Fontana J, O'Connor DS, Garcia-Cardena G, McCabe TJ, Sessa WC: Reconstitution of an endothelial nitric-oxide synthase (eNOS), hsp90, and caveolin-1 complex in vitro: evidence that hsp90 facilitates calmodulin stimulated displacement of eNOS from caveolin-1. *J Biol Chem* 275:22268–22272, 2000
18. Kitayama J, Kitazono T, Ibayashi S, Wakisaka M, Watanabe Y, Kamouchi M, Nagao T, Fujishima M: Role of phosphatidylinositol 3-kinase in acetylcholine-induced dilatation of rat basilar artery. *Stroke* 31:2487–2493, 2000
19. Gallo-Payet N, Guillon G: Regulation of adrenocortical function by vasopressin. *Horm Metab Res* 30:360–367, 1998
20. Marrero MB, Schieffer B, Paxton WG, Heerdt L, Berk BC, Delafontaine P, Bernstein KE: Direct stimulation of Jak/STAT pathway by the angiotensin II AT1 receptor. *Nature* 375:247–250, 1995
21. Saad MJ, Velloso LA, Carvalho CR: Angiotensin II induces tyrosine phosphorylation of insulin receptor substrate 1 and its association with phosphatidylinositol 3-kinase in rat heart. *Biochem J* 310:741–744, 1995
22. Velloso LA, Folli F, Sun XJ, White MF, Saad MJ, Kahn CR: Cross-talk between the insulin and angiotensin signaling systems. *Proc Natl Acad Sci U S A* 93:12490–12495, 1996
23. Prada PO, Zecchin HG, Gasparetti AL, Torsoni MA, Ueno M, Hirata AE, Corezola do Amaral ME, Hoer NF, Boschero AC, Saad MJ: Western diet modulates insulin signaling, c-Jun N-terminal kinase activity, and insulin receptor substrate 1ser307 phosphorylation in a tissue-specific fashion. *Endocrinology* 146:1576–1587, 2005
24. Eizirik DL, Welsh N, Niemann A, Velloso LA, Malaisse WJ: Succinic acid monomethyl ester protects rat pancreatic islet secretory potential against interleukin-1 beta (IL-1 beta) without affecting glutamate decarboxylase expression or nitric oxide production. *FEBS Lett* 337:298–302, 1994
25. Trinder P: Determination of blood glucose using an oxidase-peroxidase system with a non-carcinogenic chromogen. *J Clin Pathol* 22:158–161, 1969
26. Rieder MJ, Carmona R, Krieger JE, Pritchard KA Jr, Greene AS: Suppression of angiotensin-converting enzyme expression and activity by shear stress. *Circ Res* 80:312–319, 1997
27. Towbin H, Staehelin T, Gordon J: Electrophoretic transfer of proteins from polyacrylamide gels to nitrocellulose sheets: procedure and some applications. *Proc Natl Acad Sci U S A* 76:4350–4354, 1979
28. Saad MJ, Carvalho CR, Thirone AC, Velloso LA: Insulin induces tyrosine phosphorylation of JAK2 in insulin-sensitive tissues of the intact rat. *J Biol Chem* 271:22100–22104, 1996
29. Prada P, Okamoto MM, Furukawa LN, Machado UF, Heimann JC, Dolnikoff MS: High- or low-salt diet from weaning to adulthood: effect on insulin sensitivity in Wistar rats. *Hypertension* 35:424–429, 2000
30. Yamakoshi KI, Shimazu H, Togawa T: Indirect measurement of instantaneous arterial blood pressure in the rat. *Am J Physiol* 237:H632–H637, 1979
31. Priviero FM, Baracat JS, Teixeira CE, Claudino MA, DeNucci G, Antunes E: Mechanisms underlying relaxation of rabbit aorta by BAY41-2272, a nitric

oxide independent soluble guanylate cyclase activator. *Clin Exp Pharmacol Physiol* 32:728–734, 2005
32. Wyckoff MH, Chambliss KL, Mineo C, Yuhanna IS, Mendelsohn ME, Mumby SM, Shaul PW: Plasma membrane estrogen receptors are coupled to endothelial nitric-oxide synthase through $G\alpha_i$. *J Biol Chem* 276:27071–27076, 2001
33. Anter E, Thomas SR, Schulz E, Shapira OM, Vita JA, Keaney JF Jr: Activation of endothelial nitric-oxide synthase by the p38 MAPK in response to black tea polyphenols. *J Biol Chem* 279:46637–46643, 2004
34. Brandes RP, Kim D, Schmitz-Winnenthal FH, Amidi M, Godecke A, Mulsch A, Busse R: Increased nitrovasodilator sensitivity in endothelial nitric oxide synthase knockout mice: role of soluble guanylyl cyclase. *Hypertension* 35:231–236, 2000
35. Adami A, Cuzzolin L, Minuz P, Crivellente F, Lechi A, Benoni G: Vasodilating properties of a new non-steroidal anti-inflammatory drug, nitroflurbiprofen, on rat aortic rings. *Pharmacol Res* 33:239–244, 1996
36. Thirone AC, Carvalho CR, Saad MJ: Growth hormone stimulates the tyrosine kinase activity of JAK2 and induces tyrosine phosphorylation of insulin receptor substrates and Shc in rat tissues. *Endocrinology* 140:55–62, 1999
37. Carvalho CR, Carvalheira JB, Lima MH, Zimmerman SF, Caperuto LC, Amanso A, Gasparetti AL, Meneghetti V, Zimmerman LF, Velloso LA, Saad MJ: Novel signal transduction pathway for luteinizing hormone and its interaction with insulin: activation of Janus kinase/signal transducer and activator of transcription and phosphoinositol 3-kinase/Akt pathways. *Endocrinology* 144:638–647, 2003
38. Thirone AC, JeBailey L, Bilan PJ, Klip A: Opposite effect of JAK2 on insulin-dependent activation of mitogen-activated protein kinases and Akt in muscle cells: possible target to ameliorate insulin resistance. *Diabetes* 55:942–951, 2006
39. Pelicci G, Lanfrancone L, Grignani F, McGlade J, Cavallo F, Forni G, Nicoletti I, Grignani F, Pawson T, Pelicci PG: A novel transforming protein (SHC) with an SH2 domain is implicated in mitogenic signal transduction. *Cell* 70:93–104, 1992
40. Guo FF, Kumahara E, Saffen D: A CalDAG-GEFI/Rap1/B-Raf cassette couples M(1) muscarinic acetylcholine receptors to the activation of ERK1/2. *J Biol Chem* 276:25568–25581, 2001
41. Tsuneki H, Ito K, Sekizaki N, Ma EL, You Y, Kawakami J, Adachi I, Sasaoka T, Kimura I: Nicotinic enhancement of proliferation in bovine and porcine cerebral microvascular endothelial cells. *Biol Pharm Bull* 27:1951–1956, 2004
42. Kondo T, Vicent D, Suzuma K, Yanagisawa M, King GL, Holzenberger M, Kahn CR: Knockout of insulin and IGF-1 receptors on vascular endothelial cells protects against retinal neovascularization. *J Clin Invest* 111:1835–1842, 2003
43. Roberts CK, Barnard RJ, Sindhu RK, Jurczak M, Ehdaie A, Vaziri ND: A highfat, refined-carbohydrate diet induces endothelial dysfunction and oxidant/antioxidant imbalance and depresses NOS protein expression. *J Appl Physiol* 98:203–210, 2005
44. Barnard RJ, Roberts CK, Varon SM, Berger JJ: Diet-induced insulin resistance precedes other aspects of the metabolic syndrome. *J Appl Physiol* 84:1311–1315, 1998
45. Aguirre V, Werner ED, Giraud J, Lee YH, Shoelson SE, White MF: Phosphorylation of Ser307 in insulin receptor substrate-1 blocks interactions with the insulin receptor and inhibits insulin action. *J Biol Chem* 277:1531–1537, 2002
46. Aguirre V, Uchida T, Yenush L, Davis R, White MF: The c-Jun NH(2)-terminal kinase promotes insulin resistance during association with insulin receptor substrate-1 and phosphorylation of Ser(307). *J Biol Chem* 275:9047–9054, 2000
47. Abe H, Yamada N, Kamata K, Kuwaki T, Shimada M, Osuga J, Shionoiri F, Yahagi N, Kadowaki T, Tamemoto H, Ishibashi S, Yazaki Y, Makuuchi M: Hypertension, hypertriglyceridemia, and impaired endothelium-dependent vascular relaxation in mice lacking insulin receptor substrate-1. *J Clin Invest* 101:1784–1788, 1998